

# Polyaniline–Dodecylbenzene Sulfonic Acid Polymerized from Aqueous Medium: A Solid State NMR Characterization

Shifra Kababya,<sup>†</sup> Michael Appel,<sup>†</sup> Yafit Haba,<sup>‡</sup> Gregory I. Titelman,<sup>‡,§</sup> and Asher Schmidt<sup>\*,†</sup>

Department of Chemistry and Department of Chemical Engineering, Technion-Israel Institute of Technology, Haifa 32000, Israel

Received December 28, 1998; Revised Manuscript Received May 17, 1999

**ABSTRACT:** The characterization of the product of a novel polymerization procedure of aniline in aqueous medium in the presence of dodecylbenzene sulfonic acid (DBSA) as a dopant is reported. This polymerization yields stable dispersions of the emeraldine salt, which are attractive starting material for the preparation of conducting polymer blends. The as-synthesized polyaniline (PANI)–DBSA and its dedoped and redoped forms, studied by means of <sup>13</sup>C, <sup>15</sup>N, and <sup>7</sup>Li solid-state NMR and wide-angle X-ray diffraction (WAXD), reveal unusual properties. NMR and weight loss measurements show that a large portion of the dopant acid is retained upon standard dedoping by NH<sub>4</sub>OH. While this dedoped material is an insulator, NMR shows that deprotonation is incomplete and identifies residual bipolaron states. Also, the dielectric properties of the NH<sub>4</sub>OH dedoped material deviate significantly from those of fully deprotonated polyaniline and resemble those of a conducting one. Dedoping with LiOH removes a large part of the dopant acid and leads to complete deprotonation. Rotating-frame relaxation measurements indicate that the dedoped forms obtained from polyaniline–DBSA exhibit single-component behavior, implying that DBSA is molecularly mixed within the polyaniline. <sup>15</sup>N cross-polarization magic-angle spinning NMR spectra of the dedoped samples resolve two distinct imine–amine chemical species, which are formed during this particular polymerization procedure. One of the two imine–amine chemical species binds the dopant acid much stronger than the other. This is confirmed by <sup>15</sup>N{<sup>7</sup>Li} rotational-echo double-resonance (REDOR) NMR experiments on LiOH-dedoped samples. Li<sup>+</sup> cations are shown to substitute for H<sup>+</sup>s as counterions at sites from which the acid anions are not removed by deprotonation. The REDOR experiments unambiguously show that the Li<sup>+</sup> cations reside preferentially next to the imine species with the stronger DBSA binding, and within a distance of ca. 4 Å. WAXD indicates that the doped as-synthesized and dedoped powders are highly amorphous. This is attributed to the incorporation of the DBSA in the polyaniline structure.

## I. Introduction

Polyaniline (PANI, Figure 1) is one of the most promising intrinsically conducting polymers due to its straightforward polymerization, chemical and environmental stability, and relatively high conductivity. PANI is usually available as a powder of an emeraldine salt doped with mineral acids. This form has a limited processability in weakly polar or nonpolar organic solvents, which is partially overcome by redoping with organic acids,<sup>1</sup> for example by dodecylbenzene sulfonic acid (DBSA, Figure 1).<sup>2,3</sup>

Novel synthetic procedure for the preparation of PANI–DBSA by aniline polymerization in aqueous dispersion of the anilinium–DBSA complex<sup>4,5</sup> have recently been demonstrated. The synthesis<sup>5,6</sup> leads to the formation of a stable aqueous dispersion of the emeraldine salt. The stability of the aqueous PANI–DBSA dispersion is achieved by the presence of excess DBSA molecules.<sup>7</sup> Rather than improving the processability in weakly polar or nonpolar organic solvents, the possibility of maintaining PANI doped with DBSA as a stable aqueous dispersion offers an attractive starting material from which conductive blends can readily be

prepared by mixing with aqueous emulsions<sup>7</sup> or solutions<sup>4</sup> of various polymers. The characterization of the resulting doped as-synthesized PANI–DBSA emeraldine salt is the subject of this work.

Previous work<sup>5</sup> showed that when an equal volume of methanol is added to the dispersion, precipitation occurs and doped PANI–DBSA powder is obtained. However, weights of the sample before and after dedoping with aqueous NH<sub>4</sub>OH solution implied that only part of the DBSA was removed. In most other studies, when the level of dopant removal upon dedoping was investigated, it was found to be completely removed.<sup>8–11</sup> Hence, it is generally accepted that when mineral acids are used as dopants, they are totally removed upon dedoping and the resulting materials are referred to as completely deprotonated as well. As is shown by this study, this is not the case for the present PANI–DBSA system.

To characterize the PANI–DBSA system, we have prepared doped as-synthesized, NH<sub>4</sub>OH and LiOH dedoped, and HCl redoped <sup>15</sup>N-labeled samples. We employed <sup>13</sup>C, <sup>15</sup>N, and <sup>7</sup>Li solid-state NMR as the major characterization means, supplemented by weight loss and WAXD measurements. <sup>13</sup>C NMR allowed us to identify the DBSA that remains after dedoping and to study its molecular level miscibility. <sup>15</sup>N NMR on <sup>15</sup>N-labeled PANI–DBSA combined with <sup>15</sup>N{<sup>7</sup>Li} rotational-echo double-resonance (REDOR) were instrumental in revealing the unusual fine details of polyaniline itself.

\* To whom correspondence should be addressed.

<sup>†</sup> Department of Chemistry.

<sup>‡</sup> Department of Chemical Engineering.

<sup>§</sup> Present address: IMI (TAMI) Institute for Research and Development Ltd., P.O.B. 10140, Haifa 26111, Israel.

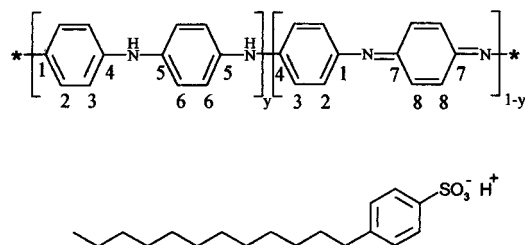


**Figure 1.** Top: polyaniline tetramer unit in the undoped state;  $(1 - y)$  denotes the degree of oxidation, with  $y = 0.5$  corresponding to the emeraldine base form. Bottom: dodecylbenzene sulfonic acid.

## II. Experimental Section

**Materials Synthesis and Sample Preparation.** The detailed polymerization procedure of aniline-DBSA in an aqueous dispersion is given elsewhere.<sup>5,7</sup> At the final stage of the polymerization, a green and stable PANI-DBSA dispersion is obtained.<sup>5-7</sup> Precipitation of the doped PANI-DBSA was induced by adding an equal volume of methanol to the aqueous dispersion. The precipitate was filtered, washed with pure methanol, and dried in a vacuum oven (60 °C, overnight). For the preparation of  $^{15}\text{N}$ -labeled samples, 2.5 g of the  $^{15}\text{N}$ -aniline (99%, Isotec Inc., Miamisburg, Ohio) and 3.5 g of the nonlabeled aniline were used to give 42% randomly  $^{15}\text{N}$ -labeled polyaniline-DBSA. This doped as-synthesized sample is denoted sample **a**.

Dedoping of PANI-DBSA was done with 1 wt % aqueous base solutions of  $\text{NH}_4\text{OH}$  or  $\text{LiOH}$ . Doped PANI (1 g) was stirred with 150 mL of the aqueous base solution for 4 h (extension up to 24 h gave the same results). The dedoped PANI powder was filtered, washed with water and aqueous base solution alternately until foaming ceased, and then dried in a vacuum oven. The samples were weighed prior to and after dedoping to record the weight loss. Two dedoped powders, denoted **b** and **c**, correspond to dedoping with  $\text{NH}_4\text{OH}$  and  $\text{LiOH}$ , respectively. A sample which was dedoped twice, first with  $\text{NH}_4\text{OH}$  and then with  $\text{LiOH}$ , is denoted sample **bc**. Dedoped samples (**b**) were also prepared with 3-fold concentration increase of the  $\text{NH}_4\text{OH}$ . Their examination by NMR, WAXD, and weight loss showed no dependence on this parameter. Also, dedoping with 1 wt % aqueous solutions of  $\text{NaOH}$  or  $\text{KOH}$  yielded the same product.

Redoping was done by immersing and stirring 1 g of sample **b** or **c** in 150 mL of 1 N  $\text{HCl}$  for 24 h at room temperature, after which the redoped PANI powder was filtered, washed with water, and dried in a vacuum oven at 60 °C, yielding green powders denoted **d** and **e**, respectively. Equivalent synthesis and preparation procedures were repeated several times with nonlabeled aniline and were examined by all techniques employed here except  $^{15}\text{N}$  NMR measurements to confirm reproducibility. An additional sample of 100%  $^{15}\text{N}$ -labeled PANI-DBSA was prepared as well and is referred to in the text.

**Apparatus and Techniques.** Conductivity measurements, using the four-point probe technique (ASTM D-991-89), were applied to compression-molded strips of PANI-DBSA. They were as follows: 0.7 S/cm for the doped as-synthesized sample **a**;  $\leq 10^{-7}$  S/cm for the dedoped samples **b** and **c**; 0.10 and 0.15 S/cm for the redoped PANI/ $\text{HCl}$  samples **d** and **e**, respectively.

**WAXD.** Wide-angle X-ray diffraction was carried out using a Philips PW 1820 X-ray diffractometer and filtered  $\text{Cu K}\alpha$  radiation ( $\lambda = 1.54 \text{ \AA}$ ). The diffractometer was operated at 40 kV and 40 mA. The diffraction patterns of PANI powders were obtained by scanning the samples in an interval of  $2\theta = 5-50^\circ$  at a rate of  $0.01^\circ/\text{s}$ .

**Solid-State NMR Spectrometer.**  $^{13}\text{C}$ ,  $^{15}\text{N}$ , and  $^7\text{Li}$  solid-state NMR measurements were carried out on a 300 MHz Chemagnetics CMX-Infinity triple-resonance spectrometer. Double-resonance measurements were done using Chemagnetics probes with 7.5 and 5.0 mm spinning modules with high-performance zirconia rotors. Triple-resonance experiments

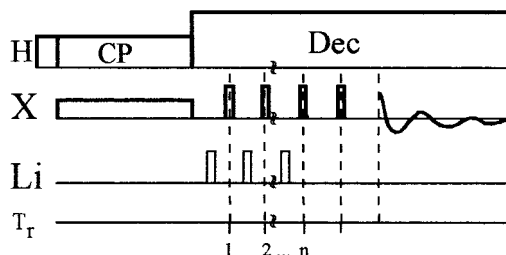


**Figure 2.**  $^{15}\text{N}\{^7\text{Li}\}$  REDOR pulse sequence. The monitored  $^{15}\text{N}$  nuclei are excited via cross-polarization. Refocusing pulses are applied every  $T_r$  on the rotor period; dephasing pulses are also applied every  $T_r$  on the half rotor period. The basic repeat sequence employs eight rotor periods with  $xy-8$  phase-cycled  $\pi$ -pulses (both refocusing and dephasing). The signal,  $S_R$ , is acquired by forming a Hahn echo simultaneously with a rotational echo after additional  $2 T_r$ . The reference signal  $S_0$  is obtained by omitting the dephasing pulses from the  $^7\text{Li}$  nuclei.

were performed using a home-built 4-channel ( $^1\text{H}-^{31}\text{P}-^{13}\text{C}-^{15}\text{N}$ ) probe<sup>12</sup> which operates with a 7.5 mm Chemagnetics spinning module, and on a 3-channel H-Y-X Chemagnetics probe with a 5 mm spinning module. Proton decoupling powers were kept at levels corresponding to 50–90 kHz, depending on the sample. For cross polarization (CP) the Hartman-Hahn match was set at 50 kHz for a duration of 1–2 ( $^{13}\text{C}$ ) or 2–5 msec ( $^{15}\text{N}$ ) to allow for optimal transferred polarization to carbon or nitrogen, respectively. Chemical shift scales of  $^{13}\text{C}$  and  $^{15}\text{N}$  are referenced to TMS and solid ammonium sulfate, respectively.  $^7\text{Li}$  was detected by either direct excitation or cross polarization. All experiments employed magic-angle spinning (MAS) with spinning speeds of 4–5 kHz, controlled to within  $\pm 2$  Hz. Spectra were obtained at room temperature.

When the conductive doped samples were measured, the NMR probe exhibited substantial detuning and increasing reflected radio-frequency (rf) power during the application of the relatively long decoupling rf irradiation.<sup>13</sup> To overcome this difficulty, rf decoupling power levels were reduced. The nonconducting sample **b** (dedoped by 1%  $\text{NH}_4\text{OH}$ ) also caused similar effects but to a much lesser extent.

**$T_{1\rho}^H$  Measurements.** Rotating-frame relaxation times,<sup>14–16</sup> in particular  $T_{1\rho}^H$  was measured indirectly by monitoring the peak intensity of the cross-polarized rare nuclei, following a proton spin-lock period with different time lengths.<sup>17</sup> The decay rates were measured by detecting (separately) the cross-polarized  $^{13}\text{C}$  and the  $^{15}\text{N}$  nuclei for samples **b** and **c** only. In the conducting samples, **a**, **d**, and **e**, these measurements were impossible due to high rf reflectance.

**REDOR.** Rotational-echo double-resonance (REDOR)<sup>18</sup> experiments served to probe interatomic proximity of up to 6 Å. In particular,  $^{15}\text{N}\{^7\text{Li}\}$ ,  $^{13}\text{C}\{^7\text{Li}\}$  and  $^{13}\text{C}\{^{15}\text{N}\}$  REDOR experiments were conducted. The REDOR pulse sequence is shown in Figure 2 for the  $^{15}\text{N}-^7\text{Li}$  pair. Following the  $^{15}\text{N}$ 's excitation, an evolution period of  $nT_r$  is introduced,  $n$  being the number of rotor cycles and  $T_r$  the rotational period of the sample. During this period,  $\pi$ -pulses are applied every rotational period to the  $^{15}\text{N}$  (observe) channel (refocusing pulses) and every half rotational period on the  $^7\text{Li}$  channel (dephasing pulses). The latter reintroduce the dipolar interaction between  $^{15}\text{N}$  and  $^7\text{Li}$  nuclei only. The phases of the  $\pi$ -pulses on each channel follow the  $xy-8$  alternation scheme.<sup>19</sup> A reference signal,  $S_0$ , is acquired when the dephasing pulses are omitted (no dipolar interaction); the REDOR signal,  $S_R$ , is acquired with the dephasing pulses. Both signals,  $S_0$  and  $S_R$ , are acquired after an additional  $2 T_r$  period which is used to form a simultaneous Hahn and rotational echo by the application of additional  $\pi$ -pulse to the  $^{15}\text{N}$  (observe) channel.

Spectral peaks of  $^{15}\text{N}$  species which possess  $\text{Li}^+$  neighbors ( $\leq 5 \text{ \AA}$ ) will be attenuated in the  $S_R$  spectrum compared to the  $S_0$  spectrum. Spectral peaks of  $^{15}\text{N}$  species without neighboring  $\text{Li}^+$  cations will display the same peak intensity in both  $S_0$  and  $S_R$ . The extent of relative peak attenuation,  $S_R/S_0$  is

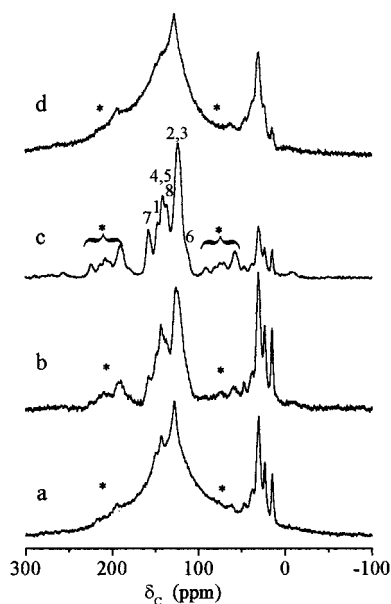


**Figure 3.**  $^{13}\text{C}$  CPMAS spectrum of 42%  $^{15}\text{N}$ -labeled PANI–DBSA. (a) Doped as-synthesized sample **a**; (b) sample **b** obtained after dedoping sample **a** with 1%  $\text{NH}_4\text{OH}$ ; (c) sample **c** obtained after dedoping sample **a** with 1%  $\text{LiOH}$ ; (d) sample **e** obtained after redoping sample **c** with 1 N  $\text{HCl}$ . The assignment of the PANI ring carbons is shown in spectrum **c** and corresponds to Figure 1. Spinning sidebands are denoted by \*. The experimental parameters are spinning speed = 5 kHz; contact time for **b** and **c** = 2 ms; and 1 ms for **a** and **d**; pulse delay = 2 s; number of transients  $\leq 6000$ ; sample weights = ca. 250 mg.

related to  $n$  and to the strength of the dipolar coupling. The latter is inversely proportional to the cube of the internuclear separation,  $r_{\text{N-Li}}^{-3}$ . REDOR spectra were collected for  $n = 8$ –48, with spinning frequencies of 4–5 kHz. Up to 16 000 transients were collected. Protons were decoupled at 50–90 kHz during the  $(n + 2)$   $T_i$  and signal acquisition periods.

In this study, our goal is restricted to identifying  $^7\text{Li}$ -coupled  $^{15}\text{N}$  species, and no attempt was made to determine the exact interatomic distances. Yet, to validate the  $^{15}\text{N}\{^7\text{Li}\}$  and  $^{13}\text{C}\{^7\text{Li}\}$  REDOR experiments, in which a spin- $1/2$  nucleus is dipolar recoupled to the spin- $3/2$   $^7\text{Li}$  nucleus,<sup>20</sup> an empirical estimate for the  $^{13}\text{C}\{^7\text{Li}\}$  dephasing behavior was obtained by a REDOR experiment on lithium–salicylate as a model compound ( $^{13}\text{C}$  was observed at its natural abundance).

### III. Results and Discussion

**Weight loss.** Weight loss upon sample dedoping is attributed solely to DBSA removal and so provides an estimate for its level of removal. The as-synthesized doped form is assumed to be an emeraldine salt with a molar ratio of PANI tetramer versus DBSA of 1:2 or less. Elemental analysis for S and N atom content of the doped samples confirms that the above ratio represents the maximal DBSA content, which can get as low as 1:1.6. Hence, the measured weight loss values after dedoping of 20% for sample **b** (1%  $\text{NH}_4\text{OH}$ ) and 55% for sample **c** (1%  $\text{LiOH}$ ) therefore reflect DBSA removal of at least 30% and 85%, respectively. Clearly, the quantity of DBSA retained in sample **b** is much higher than that in sample **c**.

**$^{13}\text{C}$  Measurements.**  $^{13}\text{C}$  CPMAS NMR spectra were recorded for the four types of PANI–DBSA samples and are shown in Figure 3. In the spectrum of the doped as-synthesized sample **a** (lowest trace), we distinguish two main chemical shift regions. The ring carbon region centered at 130 ppm is heterogeneously broadened<sup>21,22</sup>

and spread over ca. 250 ppm; this region has contributions from all of the PANI carbons and from the aromatic ring of the DBSA. The aliphatic carbon region spreads between 10–50 ppm; it consists of relatively narrow peaks which arise solely from the aliphatic DBSA chains.

The envelope of the broadened aromatic peak region is endowed with small narrow peaks, e.g. at 143.5 ppm. The latter originate from residual anilinium–DBSA complex, as is confirmed below by the  $^{15}\text{N}$  results. The spectrum of sample **b** (Figure 3b) exhibits substantial narrowing of the aromatic peaks upon dedoping with  $\text{NH}_4\text{OH}$ , now being confined to the 105–165 ppm region (first-order spinning sidebands are resolved and marked by \*). The presence of intense aliphatic peaks in the spectrum proves that DBSA remains in a high concentration even after the dedoping process, in accord with the weight loss results. The spectrum of sample **c** (Figure 3c), compared with that of **b**, shows further narrowing of the peaks in the aromatic region, giving rise to a finely structured spectrum. In the latter, the peaks of all different carbon species are partially resolved. The assignment of all peaks in the aromatic region is in agreement with Kaplan et al.<sup>22</sup> and is shown in Figure 3c above the  $^{13}\text{C}$  CPMAS spectrum of sample **c**. The much lower relative intensity of the aliphatic peaks of sample **c** compared to those of sample **b**, indicates that more DBSA is removed upon dedoping with  $\text{LiOH}$ , in agreement with the weight loss results. The aromatic peaks of the remaining DBSA, being of much smaller relative quantity, are not resolved among the aromatic PANI peaks.<sup>23</sup>

Samples **b** and **c** were redoped with  $\text{HCl}$  yielding the conducting ( $\sigma \approx 0.10$  and  $0.15$  S/cm) samples **d** and **e**, respectively. The spectrum of sample **e** (Figure 3d), reproduces the overall spectral features of sample **a**, except for two subtle changes which occur due to DBSA and residual anilinium–DBSA complex removal: (a) the (small) sharp spectral features in the aromatic peak region are diminished, and (b) the broadening of the aliphatic peaks can now be observed. These experimental results (spectrum, conductivity, and brown to green color change) verify that the dedoping procedures undertaken here, in particular the  $\text{LiOH}$  dedoping, are reversible. In addition, the broadening observed for the aliphatic peaks of the redoped samples **e** and **d**, suggests that the aliphatic chains also are affected by the same heterogeneous broadening mechanism which governs the line width of the aromatic peaks. Yet, this broadening is less pronounced than that for the aromatic carbons. This broadening of the aliphatic chains of DBSA and the fact that its ring carbons do not display narrow peaks in the spectra of the  $\text{HCl}$ -redoped samples imply that the DBSA which remains after dedoping co-participates as a dopant together with the hydrochloric acid.

**$^{15}\text{N}$  Measurements.**  $^{15}\text{N}$  CPMAS spectra of the 42%  $^{15}\text{N}$ -labeled samples are shown in Figure 4. The doped as-synthesized sample **a**, displays two heterogeneously broadened peaks (lower trace) which spread between 30 and 600 ppm (Figure 4a). The amines and the protonated imines give rise to two spectral features which are not resolved: a 130 ppm wide amines peak at the high-field end at  $\sim 100$  ppm and an ultrabroad protonated imines peak that covers unevenly the entire  $\sim 600$  ppm range and tails off towards the low-field end. It should be noted that in the few former studies which



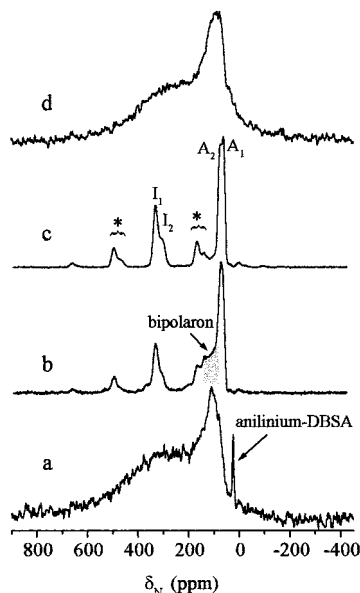


**Figure 4.**  $^{15}\text{N}$  CPMAS spectrum of 42%  $^{15}\text{N}$ -labeled PANI-DBSA. (a) Doped as-synthesized sample **a**; (b) sample **b** obtained after dedoping sample **a** with 1%  $\text{NH}_4\text{OH}$ ; (c) sample **c** obtained after dedoping sample **a** with 1%  $\text{LiOH}$ ; (d) sample **e** obtained after redoping sample **c** with 1 N  $\text{HCl}$ . Amines and imines are denoted by A and I, respectively, and spinning sidebands are denoted by \*. The experimental parameters are spinning speed = 5 kHz; contact time = 2 ms; pulse delay = 1 s; number of transients  $\leq 8000$ .

utilized  $^{15}\text{N}$  NMR to characterize differently prepared ( $^{15}\text{N}$ -labeled) PANI systems<sup>24,13</sup> a much smaller spread of nitrogen chemical shifts ( $<300$  ppm) was observed in the doped state. This line broadening was suggested by Kaplan et al.<sup>22</sup> to originate from variations in charge density along the polymer backbone due to heterogeneity in the polyaniline packing and conformational multiplicity. The extensive broadening in the PANI-DBSA system is attributed to the higher packing disorder imparted by the bulky aliphatic chains of DBSA. An additional sharp peak observed at 26 ppm belongs to the residual anilinium-DBSA complex, and is estimated to represent less than 2% of the total integrated intensity of the spectrum. Its assignment was confirmed by the  $^{15}\text{N}$  CPMAS spectrum of the crystalline 42%  $^{15}\text{N}$ -labeled anilinium-DBSA complex. This residual complex is entirely removed following dedoping, as is evident from the spectra of samples **b**, **c**, and **e** (Figure 4b–d). Sample **e**, obtained after a dedoping-redoping cycle of sample **a**, displays a spectrum (Figure 4d) similar to that of **a**, except for the 26 ppm peak of anilinium-DBSA which is removed. The spectrum obtained for sample **d** ( $\text{NH}_4\text{OH}$ -dedoped and  $\text{HCl}$ -redoped) is practically identical to that of **e**. The reproducibility of the extensive  $^{15}\text{N}$  line width by  $\text{HCl}$  redoping, implies that the heterogeneities that give rise to this broadening are frozen into the polyaniline framework even after substantial removal of the DBSA. It should also be noted that there is no residual emeraldine-base form (undoped) present in the doped samples, as is clearly attested by their  $^{15}\text{N}$  spectra in Figure 1a,d.

Next, we focus on the  $^{15}\text{N}$  CPMAS spectrum of sample **c** (dedoped by  $\text{LiOH}$ ) shown in Figure 4c. This spectrum shows two partially resolved imine peaks and two partially resolved amine peaks with the following chemical shifts: amines,  $A_1$  and  $A_2$  at 61.0 and 71.5 ppm, and imines,  $I_1$ , and  $I_2$  at 328.0, and 302.5 ppm.

Careful inspection of the spectrum of sample **b** (Figure 4b), also reveals the presence of these distinct spectral features but with different peak ratios: the inner peaks,  $A_2$  and  $I_2$ , are of relatively weaker intensity in comparison with the outer ones,  $A_1$  and  $I_1$ . This is confirmed by deconvolution of the imine peaks of samples **b** and **c**. Moreover, this sample, which was dedoped by  $\text{NH}_4\text{OH}$ , exhibits an additional broad spectral component at 100–140 ppm. Since this broad peak overlaps with imine spinning sidebands, the experiment was repeated with a 4 kHz spinning speed, resolving clearly the 100–140 ppm peak (not shown). On the basis of previous studies<sup>24,25</sup> this component is identified to arise from (positively) charged protonated imines which constitute residual bipolaron states and their adjacent amines. To date, there is only one report on the presence of charged protonated imines in *dedoped* PANI.<sup>25</sup> In this report, Wherle et al.<sup>25</sup> studied polyaniline which was prepared by electro-polymerization under highly acidic conditions (3 M  $\text{HClO}_4$ ). The dedoped sample, obtained by discharge in acetonitrile, gave rise to a  $^{15}\text{N}$  peak at the same chemical shift found by us (100–140 ppm), and its assignment was based on chemical shifts of model compounds. Espe et al.<sup>24</sup> also assign this chemical shift range to the charged protonated imines which they observe in the emeraldine salt of  $\text{HF}$ -doped PANI; their assignment relies on an earlier study of model compounds.<sup>26</sup>

The tight incorporation of DBSA in the PANI framework not only inhibits its removal but also prevents complete deprotonation of the imines by dedoping with  $\text{NH}_4\text{OH}$ . In addition to the incomplete deprotonation that results in remaining bipolaron states, sample **b** detunes the NMR probe (in contrast to the  $\text{LiOH}$ -dedoped sample), and during rf irradiation, it exhibits rf-reflectance patterns that resemble those of conducting samples. These facts imply that the dielectric properties of this sample strongly deviate from those of an insulator, even though its bulk conductivity is practically zero.

When the  $\text{NH}_4\text{OH}$ -dedoped sample undergoes a second consecutive dedoping step, by  $\text{LiOH}$  (sample **bc**), the peaks of the protonated imines (bipolaron states) vanish. Their intensity is transferred mainly to the  $A_2$  and  $I_2$  peaks, leading to a spectrum (not shown) similar to that of sample **c**. Therefore, the dedoping by the two consecutive steps described above, and the single-step  $\text{LiOH}$ -dedoping, both yield the same product.

It should be emphasized that the spectra of both  $\text{NH}_4\text{OH}$ - and  $\text{LiOH}$ -dedoped PANI display peaks of the two chemical species for which only their relative intensities depend on the dedopant. The chemical identity of these species, as reflected by their fixed chemical shifts, suggests that the different environments originate in the as-synthesized polymer itself. If these species were identical in the doped as-synthesized material, it is likely that they would remain indistinguishable after dedoping.

The experimental findings so far can be summarized as follows: The  $A_1$ – $I_1$  species emerges predominantly by treatment with  $\text{NH}_4\text{OH}$ , accompanied by minor DBSA removal. Dedoping with  $\text{LiOH}$  exposes predominantly the  $A_2$ – $I_2$  species, along with substantial DBSA removal. Consecutive  $\text{LiOH}$  dedoping deprotonates the residual bipolaron states and removes DBSA; moreover, the peaks associated with the bipolarons are converted mostly to peaks associated with the  $A_2$ – $I_2$  species. These findings allow the discrimination of the two dedopants

in terms of “weak” ( $\text{NH}_4\text{OH}$ ) and “strong” ( $\text{LiOH}$ ) dedopants. This discrimination is supported by previous studies,<sup>27,28</sup> which reported the high efficiency of  $\text{LiOH}$  in solvating and breaking hydrogen bonds in polyanilines. By inference, this discrimination can be extended to the chemical species being preferentially exposed upon dedoping. The  $\text{A}_1\text{--I}_1$  exposed by the weak dedopant, and  $\text{A}_2\text{--I}_2$  exposed by the strong dedopant, correspond to species possessing weak and strong DBSA binding affinities, respectively.

Richter et al.<sup>29</sup> identified similar spectral features (chemical shifts) in dedoped ( $^{15}\text{N}$ -labeled) PANI prepared by various polymerization procedures. Using solution-state and solid-state  $^{15}\text{N}$  NMR on model compounds, Richter proposed that such spectral features in the emeraldine base may reflect variations in the polymer chain sequencing which result from changes in the degree of oxidation. Nevertheless, the authors indicate that their experimental data are not sufficient to substantiate this assignment. Adams et al.<sup>13</sup> detected an amine peak splitting of 5.9 ppm for an oriented film of emeraldine base cast from *N*-methyl-2-pyrrolidinone (NMP). Whether this splitting is induced by ordering or by solvent effect could not be determined. So far, it is only this PANI–DBSA which displayed this combination of the  $\text{A}_1\text{--I}_1$  and  $\text{A}_2\text{--I}_2$  peaks coexisting.

Recently, polyanilines undergoing gradual protonation-deprotonation cycles by mineral and organic acids under controlled acidity-basicity conditions were studied by X-ray photoelectron spectroscopy (XPS).<sup>30–32</sup> In these studies, the common oxidative polymerization was employed with either  $\text{HCl}$  or  $\text{H}_2\text{SO}_4$ . Also in these studies,<sup>30</sup> the organic acids (and DBSA in particular) showed high retention tendency upon dedoping and high relative affinity upon redoping. The high retention of DBSA was attributed to its bulkiness. The  $\text{N}(1s)$  XPS spectral analyses employed deconvolution procedure which required two different charged nitrogen peaks, instead of the anticipated uniform distribution of binding energies. It is possible that the implication for the presence of two distinct chemical species exists also in these systems, in a fashion similar to those shown in our work. To further delineate the nature of these two chemically differing groups displayed by the PANI–DBSA system, relaxation measurements and REDOR experiments were conducted and are described below.

**$T_{1\rho}^{\text{H}}$  Measurements.** Rotating-frame relaxation measurements, in particular  $T_{1\rho}^{\text{H}}$ , can provide information on the miscibility and uniformity of multicomponent polymeric systems at the molecular level, as well as an estimate of the domain sizes.<sup>14–16</sup> The decay of the spin-locked proton magnetization was measured by detecting (separately)  $^{13}\text{C}$  and  $^{15}\text{N}$  cross-polarized signals. Figure 5 shows this decay as monitored by the  $^{15}\text{N}$  amine and imine peaks for samples **b** and **c**. For sample **b**, only the peaks of  $\text{A}_1$  and  $\text{I}_1$  were sufficiently intense to be monitored. The measured  $T_{1\rho}^{\text{H}}$  values for all ring carbons and for both amine and imine nitrogens were found to be identical within a particular sample. No bi- or multiexponential components were detected within the experimental accuracy. The  $T_{1\rho}^{\text{H}}$  values measured for samples **b** and **c** and the crystalline anilinium–DBSA complex are summarized in Table 1.

In each dedoped sample (**b** or **c**), both the DBSA aromatic rings and those of the benzoid and quinoid PANI rings possess indistinguishable  $T_{1\rho}^{\text{H}}$  values. The DBSA ring carbons fully adopt the relaxation behavior

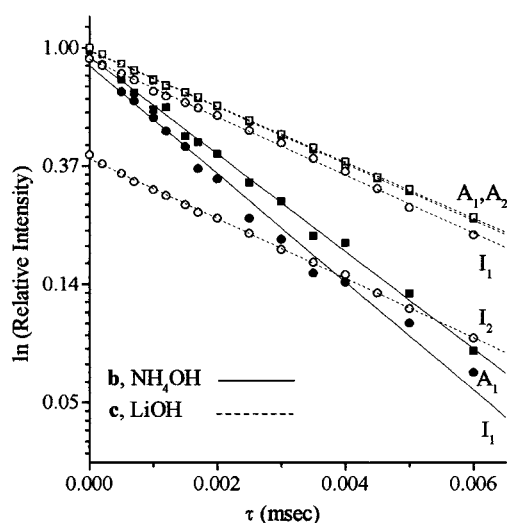


**Figure 5.** Proton spin-locked magnetization decay of the dedoped samples **b** and **c**. These are monitored by the amine (squares) and imine (circles) peak intensities following cross polarization. The experimental parameters are spinning speed = 5 kHz; contact time = 5 ms; pulse delay = 1 s; number of transients  $\leq 2000$ . Filled symbols denote sample **b**, and empty symbols denote sample **c**. Experimental data points on the semilogarithmic plot were fit by a linear regression.

**Table 1. Proton Rotating-Frame Relaxation**

sample	$T_{1\rho}^{\text{H}}$ (msec)
PANI–DBSA dedoped with $\text{NH}_4\text{OH}$ ( <b>b</b> )	$2.0 \pm 0.2$
PANI–DBSA dedoped with $\text{LiOH}$ ( <b>c</b> )	$4.5 \pm 0.2$
anilinium–DBSA complex	$10.0 \pm 0.2$

of the polyaniline chain, implying that the PANI and the DBSA are mixed on a molecular level.<sup>33</sup> These results suggest that the sulfonate–aromatic rings of DBSA are fully compatibilized at the molecular level within the PANI chain structure, possibly forming strong molecular interactions. The measured  $T_{1\rho}^{\text{H}}$  values of the aliphatic carbons of the DBSA shorten gradually by 0.3–0.5 ms as they get farther away from the aromatic ring, reflecting increased mobility of the DBSA chain. Since DBSA is a liquid at room temperature, we include the  $T_{1\rho}^{\text{H}}$  value of the complex of anilinium–DBSA as a reference for a rigid crystalline solid.

The longer  $T_{1\rho}^{\text{H}}$  value resulting after dedoping by  $\text{LiOH}$  (**c**, 4.5 ms) versus  $\text{NH}_4\text{OH}$  (**b**, 2 ms) is interpreted in terms of a tighter and more rigid packing. The substantial removal of DBSA from the PANI framework upon dedoping with  $\text{LiOH}$  allows it to form a more compact structure. This evidence further substantiates the understanding that DBSA influences the PANI structure in each of its forms. Moreover, since the two distinct chemical species which are identified by the  $^{15}\text{N}$  spectra do not show different  $T_{1\rho}^{\text{H}}$  values (Figure 5), they do not represent separate domains<sup>33</sup> with size larger than 50 Å. Thus, the polyaniline chains are constructed of interleaved *chemical species*,  $\text{A}_1\text{--I}_1$  and  $\text{A}_2\text{--I}_2$ , which alternate every one or two tetramer units.

The doped samples (**a**, **d**, and **e**) caused severe probe detuning and diverging rf reflectance; therefore reliable relaxation measurements were impossible.

**WAXD.** To further assess the structural characteristics of PANI–DBSA in its different states, wide-angle X-ray diffraction spectra were measured for samples **a–c** and are shown in Figure 6. All three forms of PANI–DBSA exhibit a broad amorphous peak with

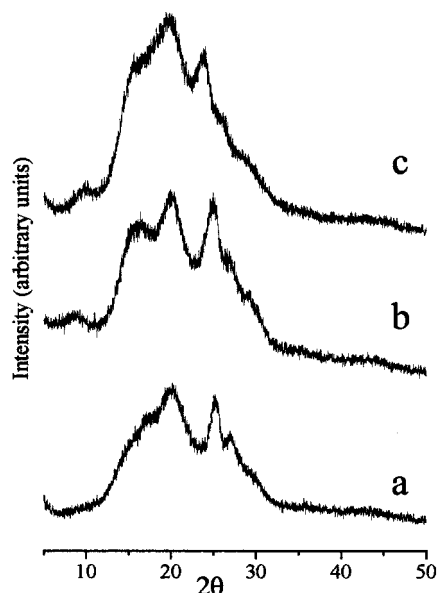


**Figure 6.** WAXD spectra of PANI-DBSA. (a) Doped as-synthesized sample **a**; (b) sample **b** obtained after dedoping sample **a** with 1%  $\text{NH}_4\text{OH}$ ; (c) sample **c** obtained after dedoping sample **a** with 1%  $\text{LiOH}$ .

relatively wide reflection peaks on top of it. These are interpreted in terms of low crystallinity and a broad distribution of d-spacings and attributed to the interference of DBSA within the polyaniline structure. More detailed examination of the three spectra shows only small differences between the doped as-synthesized and the  $\text{NH}_4\text{OH}$ -dedoped samples, both possessing high DBSA content. The differences become more pronounced as we move to the  $\text{LiOH}$ -dedoped sample, which displays both higher crystallinity and peak shifts. In this sample (**c**), the substantial DBSA-removal allows a small rearrangement, thus forming a more ordered and compact packing. This change is also alluded to by the relaxation measurements.

**REDOR Measurements.** After  $\text{LiOH}$  dedoping (**c** or **bc**), at most 15% of the DBSA remains bound in the deprotonated PANI framework. Therefore, the negatively charged DBSA anions must be counterbalanced by the  $\text{Li}^+$  cations; i.e., the polyaniline and the strongly bound DBSA act as a "cation exchanger", releasing  $\text{H}^+$  in favor of  $\text{Li}^+$ . The presence of the  $\text{Li}^+$  cations in **c** or **bc** is easily verified via  $^7\text{Li}$ -MAS NMR (inset of Figure 8) and can be utilized now to report on their new chemical environments. Since the  $^7\text{Li}$  chemical shift is rather insensitive, the REDOR technique is tailored to detect its location within the PANI-DBSA framework. The  $48\ T_r\ ^{15}\text{N}\{^7\text{Li}\}$  REDOR spectra of **c** are shown in Figure 7. The lower traces show an overlay of two spectra: a Hahn-echo reference spectrum,  $S_0$  (solid line), and a REDOR dephased spectrum,  $S_R$  (dashed line). In the latter, since the dipolar interaction is reintroduced, peaks of  $^{15}\text{N}$  species which possess neighboring  $\text{Li}^+$  cations (within ca. 5 Å) are attenuated. It is therefore instructive to plot the difference spectrum (Figure 7, top trace),  $S_0 - S_R$ , in which peaks appear only for those species with neighboring lithium cations.  $I_2$  displays the most intense difference peak, whereas  $A_2$  has a smaller one. It should be noted that the selectivity exhibited by the difference peak of  $I_2$  is emphasized by the fact that the reference peak of  $I_2$  is about half that of  $I_1$ . This result indicates that the lithium cations reside preferentially in the vicinity of the  $A_2$ - $I_2$  species and closer

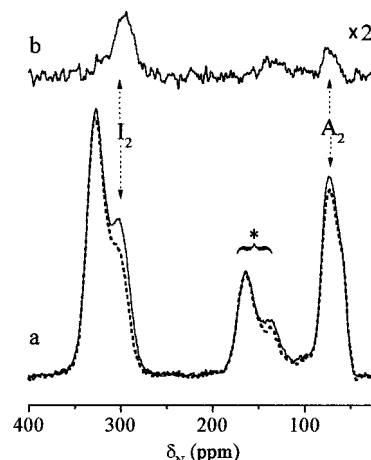


**Figure 7.**  $48\ T_r\ ^{15}\text{N}\{^7\text{Li}\}$  REDOR spectra of 42%  $^{15}\text{N}$ -labeled PANI-DBSA sample **c**. The lower traces show an overlay of the full echo spectrum ( $S_0$ , thick line) and the REDOR dephased spectrum ( $S_R$ , dashed line). The difference spectrum,  $S_0 - S_R$ , shown by the upper trace, clearly displays a peak at the  $I_2$  position and a weaker peak at the  $A_2$  position. Samples were spun at 5 kHz spinning speed, and a contact time of 5 ms was employed. The longer contact time favors the imine peaks versus amines; 16000 scans were collected.

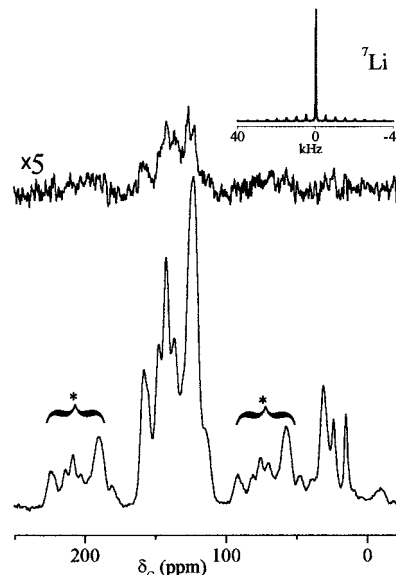


**Figure 8.**  $16\ T_r\ ^{13}\text{C}\{^7\text{Li}\}$  REDOR spectra of sample **c**. The reference spectrum ( $S_0$ ) and the difference spectrum ( $S_0 - S_R$ ) are shown by the lower and upper traces, respectively. Nonselective difference peaks of all ring carbons are exhibited. Samples were spun at 5 kHz spinning speed, and a contact time of 2 ms was employed. 10 000 scans were collected. The inset shows a  $^7\text{Li}$  MAS spectrum of sample **c** obtained by single pulse excitation and proton decoupling. Spinning was at 5 kHz, and 512 scans were acquired with a 1 s pulse delay.

to the  $I_2$  imine among this group. The estimated  $I_2$ - $\text{Li}^+$  distance is about 4 Å.

Considering the geometrical constraints implied by the proximity of the  $\text{Li}^+$  cation to the specific  $I_2$ - $A_2$  pair, similar proximity to the PANI ring carbons should be found. This is indeed confirmed by a  $^{13}\text{C}\{^7\text{Li}\}$  REDOR experiment conducted on **c**, as shown in Figure 8. Since the  $^{13}\text{C}$  spectra lack the sensitivity to distinguish between the two chemical species, their  $^{13}\text{C}\{^7\text{Li}\}$  REDOR spectrum shows a nonselective attenuation of all ring carbon peaks, as expected.

This observation complements the earlier ones: the  $A_2$ - $I_2$  groups are identified as those with the higher



affinity to DBSA compared with the  $A_1$ – $I_1$  groups. The  $A_2$ – $I_2$  groups inhibit the removal of DBSA and partially succeed in maintaining their imines in a protonated form after  $NH_4OH$  dedoping. When DBSA remains bound even after dedoping by  $LiOH$ , the  $Li^+$  cations exchange  $H^+$  cations as counterions, bridging the DBSA sulfonate group with the  $I_2$  imines. The molecular-level mixing of the DBSA within the PANI framework as inferred from the  $T_{1\rho}^H$  measurements, is now visualized in terms of molecular contacts and interactions between functional groups.

#### IV. Conclusions

Detailed solid-state NMR characterization of the PANI–DBSA system reveals structure and properties which deviate from PANI systems that have been studied so far. We find that the specific synthetic procedure employed here, aniline polymerized in the presence of DBSA in aqueous medium, leads to the formation of emeraldine salt with new characteristics. The DBSA strongly interacts with the imine groups on the polyaniline, thus limiting its removal by standard dedoping procedures as is indicated by weight loss measurements and  $^{13}C$  NMR. The resulting dedoped forms of PANI–DBSA are found by  $T_{1\rho}^H$  measurements, to incorporate DBSA in the PANI framework as a uniform homogeneous single-phase material. Using  $^{15}N$  NMR, which is by far more sensitive and less complex than  $^{13}C$  NMR, we identify in the dedoped samples the presence of two distinct chemical species of amines and imines, denoted as  $A_1$  and  $A_2$  and as  $I_1$  and  $I_2$ ; respectively. We find that these species can crudely be grouped into  $A_1$ – $I_1$  and  $A_2$ – $I_2$ . The first group is formed predominantly upon standard dedoping by  $NH_4OH$ , which leaves a large portion (~70%) of the DBSA bound to the polyaniline. The second emerges when the more powerful dedopant,  $LiOH$ , is used, thus forcing out a substantial portion of the DBSA (~85%). The high efficiency of lithium cations in solvating and breaking hydrogen bonds was recently reported.<sup>27,28</sup>

Thus, the PANI–DBSA emeraldine salt constitutes a framework in which the DBSA is attached by intermolecular forces, possibly hydrogen bonding and other electrostatic interactions. These, in turn, inhibit dopant removal as well as deprotonation in the  $NH_4OH$  case. The  $^{15}N$  spectra reveal that deprotonation is incomplete and identify a residual quantity of charged protonated imines as bipolaron states. While bulk conductivity is totally switched off by the  $NH_4OH$  dedoping, NMR probe detuning and rf reflectance indicate that this powder maintains dielectric properties which are typical of conducting samples. Dedoping with  $LiOH$  results in complete deprotonation.

Our experimental findings imply that the distinct chemical species are formed during the synthesis itself and are a characteristic of the doped as-synthesized PANI–DBSA. Their detection by  $^{15}N$  NMR is possible only after dedoping. Moreover, they also suggest that the two species found differ in their DBSA binding affinity, with  $A_1$ – $I_1$  having a lower affinity than that of  $A_2$ – $I_2$ . Direct evidence which substantiates such a discrimination between the amine–imine species was obtained by employing  $^{15}N\{^7Li\}$  REDOR experiment on samples dedoped by  $LiOH$ . In the latter, adjacent to the remaining 15% DBSA anions,  $Li^+$  cations replace  $H^+$  as counterions and so served to probe their immediate PANI vicinity. The REDOR experiment locates the  $Li^+$

cations near the  $A_2$ – $I_2$  pairs and closer to the  $I_2$  than to the  $A_2$ . The preferred formation of the  $A_2$ – $I_2$  groups only after DBSA is forced out by  $LiOH$  dedoping and the exclusive selectivity of the  $I_2$  imine as the lithium cation site confirm their identification as two chemically distinct species, having weak and strong DBSA binding affinities. In view of the relaxation measurements that exclude phase separation, we can assume that these groups ( $A_1$ – $I_1$  and  $A_2$ – $I_2$ ) must alternate within one or two tetramer units. WAXD indicated that the PANI–DBSA structures are highly amorphous, as may be dictated by the incorporation of the DBSA within the polyaniline framework. Moreover, the heterogeneities resulting from the synthesis appear to be frozen into this framework even after substantial DBSA removal by  $LiOH$  dedoping. These heterogeneities are manifested by the reoccurrence of the broad  $^{15}N$  line shapes in the redoped samples. Last, the strong PANI–DBSA interactions as evidenced in this work and the high affinity between PANI and aromatic sulfonate acids as reported by Neoh et al.,<sup>30</sup> suggest that both the aromatic ring and the polar sulfonate group of the dopants constitute the binding. The first leads to hydrophobic interactions, and the second to electrostatic ones.

**Acknowledgment.** The authors thank Prof. M. Narkis from Chemical Engineering, Technion, and Prof. A. Siegmann from Materials Engineering, Technion, for permission to use their new polymerization procedure of aniline–DBSA in aqueous dispersions, developed in the Chemical Engineering Laboratories, and for fruitful discussions. A.S. also thanks Prof. J. Schaefer and Eng. R.A. McKay for their kind assistance in the construction of the four-channel probe. This research was supported in part by the Israel Science Foundation founded by the Israel Academy of Sciences & Humanities (290/95, 9031/96) and by the Fund for the Promotion of Research at the Technion.

#### References and Notes

- (1) Cao, Y.; Smith, P.; Heeger, A. J. *Synth. Met.* **1993**, 55–57, 3514.
- (2) Titelman, G. I.; Zilberman, M.; Siegmann, A.; Haba, Y.; Narkis, M. *J. Appl. Polym. Sci.* **1997**, 66, 2199.
- (3) Roichman, Y.; Silverstein, M. S.; Siegmann, A.; Narkis, M. *J. Macromol. Phys. Ed.* **1999**, B38, 145.
- (4) Gospodinova, N.; Mokreva, P.; Tdanov, T.; Terlemezyan, L. *Polymer* **1997**, 38, 743.
- (5) Haba, Y.; Titelman, G. I.; Segal, E.; Narkis, M.; Siegmann, A. *Synth. Met.* **1999**, in press.
- (6) Haba, Y. M.Sc. Dissertation, Department of Chemical Engineering, Technion, Haifa, Israel, 1998.
- (7) Haba, Y.; Titelman, G. I.; Segal, E.; Narkis, M.; Siegmann, A. *Synth. Met.* **1999**, submitted for publication.
- (8) Huang, W. S.; Humphrey, B. D.; MacDiarmid, A. G. *J. Chem. Soc. Faraday Trans.* **1986**, 82, 2385.
- (9) MacDiarmid, A. G.; Chiang, J. C.; Richter, A. F.; Epstein, A. J. *Synth. Met.* **1987**, 18, 285.
- (10) Kenwright, A. M.; Feast, W. J.; Adams, P. N.; Milton, A. J.; Monkman, A. P.; Say, B. J. *Polymer* **1992**, 33, 4292.
- (11) Asturias, G. E.; MacDiarmid, A. G.; McCall, R. P.; Epstein, A. J. *Synth. Met.* **1989**, 29, E157.
- (12) McKay, R. A. U.S. Patent 4,446,431 May 1, **1984**.
- (13) Adams, P. N.; Apperley, D. C.; Monkman, A. P. *Polymer* **1993**, 34, 328.
- (14) Stejskal, E. O.; Schaefer, J.; Sefick, M. D.; McKay, R. A. *Macromolecules* **1981**, 14, 275.
- (15) Mehring, M. *High-Resolution NMR Spectroscopy in Solids*; Springer-Verlag: Berlin, 1976; Volume 11, Chapter 4.
- (16) Connor, T. M. *High-Resolution NMR Spectroscopy in Solids*; Springer-Verlag: Berlin 1971; Volume 4, page 247.
- (17) Pines, A.; Shattuck, T. W. *J. Chem. Phys.* **1974**, 61, 1255.
- (18) Gullion, T.; Schaefer, J. *J. Magn. Reson.* **1989**, 81, 196.

- (19) Gullion, T.; Baker, D. B.; Conradi, M. S. *J. Magn. Reson.* **1990**, *89*, 479.
- (20) Gee, B.; Janssen, M.; Eckert, H. *J. Non.-Cryst. Solids* **1997**, *41*, 215.
- (21) Kaplan, S.; Conwell, E. M.; Richter, A. F.; MacDiarmid, A. G. *Synth. Met.* **1989**, *29*, E235.
- (22) Kaplan, S.; Conwell, E. M.; Richter, A. F.; MacDiarmid, A. G. *J. Am. Chem. Soc.* **1988**, *110*, 7647.
- (23) Selective observation of the DBSA ring carbons was achieved by a 64  $T_r$   $^{13}\text{C}\{^{15}\text{N}\}$  REDOR experiment on a 100%  $^{15}\text{N}$ -labeled PANI-DBSA dedoped by  $\text{NH}_4\text{OH}$ .
- (24) Espe, M. P.; Mattes, B. R.; Schaefer, J. *Macromolecules* **1997**, *30*, 6307.
- (25) Wehrle, B.; Limbach, H. H.; Mortensen, J.; Heinze, J. *Angew. Chem., Int. Ed. Engl. Adv. Mater.* **1989**, *28*, 1741.
- (26) Botto, R. E.; Roberts, J. D. *J. Org. Chem.* **1979**, *44*, 140.
- (27) Angelopoulos, M.; Liao, Y. H.; Furman, B.; Graham, T. *Macromolecules* **1996**, *29*, 3046.
- (28) Angelopoulos, M.; Dipietro, R.; Zheng, W. G.; MacDiarmid, A. G.; Epstein, A. J. *Synth. Met.* **1997**, *84*, 35.
- (29) Richter, A. F.; Ray, A.; Ramanathan, K. V.; Manohar, S. K.; Furst, G. T.; Opella, S. J.; MacDiarmid, A. G.; Epstein, A. J. *Synth. Met.* **1989**, *29*, E243.
- (30) Neoh, K. G.; Pun, M. Y.; Kang, E. T.; Tan, K. L. *Synth. Met.* **1995**, *73*, 209.
- (31) Neoh, K. G.; Pun, M. Y.; Kang, E. T.; Tan, K. L. *J. Poly. Sci., Polym. Phys.* **1995**, *33*, 833.
- (32) Kang, E. T.; Neoh, K. G.; Tan, K. L. *Polymer* **1996**, *37*, 925.
- (33) Veeman, W. S.; Mass, W. E. J. R. *Solid State NMR Techniques for the Study of Polymer-Polymer Miscibility*; Springer-Verlag 1994; Volume 32, p 127-172.

MA982010E